Fermi National Accelerator Laboratory

FERMILAB-Pub-89/229-E
[E-741/CDF]

The Two Jet Invariant Mass Distribution at $\sqrt{s}$ = 1.8 TeV*

F. Abe[16] D. Amidei[3], G. Apollinari[11], G. Ascoli[7], M. Atac[4], P. Auchincloss[14], A.R. Baden[6], A. Barbaro-Galtieri[9], V.E. Barnes[12], F. Bedeschi[11], S. Behrends[12], S. Belforte[11], G. Bellettini[11], J. Bellinger[17], J. Bensinger[2], A. Beretvas[14], P. Berge[4], S. Bertolucci[5], S. Bhadra[7], M. Binkley[4], R. Blair[1], C. Blocker[2], J. Bofill[4], A.W. Booth[4], G. Brandenburg[6], D. Brown[6], A. Byon[12], K.L. Byrum[17], M. Campbell[3], R. Carey[6], W. Carithers[9], D. Carlsmith[17], J.T. Carroll[4], R. Cashmore[4], F. Cervelli[11], K. Chadwick[4,12], T. Chapin[13], G. Chiarelli[11], W. Chinowsky[9], S. Cihangir[15], D. Cline[17], D. Connor[10], M. Contreras[2], J. Cooper[4], M. Cordelli[5], M. Curatolo[5], C. Day[4], R. DelFabbro[11], M. Dell'Orso[11], L. DeMortier[2], T. Devlin[14], D. DiBitonto[15], R. Diebold[1], F. Dittus[4], A. DiVirgilio[11], J.E. Elias[4], R. Ely[9], S. Errede[7], B. Esposito[5], B. Flaugher[14], E. Focardi[11], G.W. Foster[4], M. Franklin[6,7], J. Freeman[4], H. Frisch[3], Y. Fukui[8], A.F. Garfinkel[12], P. Giannetti[11], N. Giokaris[13], P. Giromini[5], L. Gladney[10], M. Gold[9], K. Goulianos[13], C. Grosso-Pilcher[3], C. Haber[9], S.R. Hahn[10], R. Handler[17], R.M. Harris[9], J. Hauser[3], T. Hessing[15], R. Hollebeek[10], P. Hu[14], B. Hubbard[9], P. Hurst[7], J. Huth[4], H. Jensen[4], R.P. Johnson[4], U. Joshi[14], R.W. Kadel[4], T. Kamon[15], S. Kanda[16], D.A. Kardelis[7], I. Karliner[7], E. Kearns[6], R. Kephart[4], P. Kesten[2], H. Keutelian[7], S. Kim[16], L. Kirsch[2], K. Kondo[16], U. Kruse[7], S.E. Kuhlmann[12], A.T. Laasanen[12], W. Li[1], T. Liss[3], N. Lockyer[10], F. Marchetto[15], R. Markeloff[17], L.A. Markosky[17], P. McIntyre[15], A. Menzione[11], T. Meyer[15], S. Mikamo[8], M. Miller[10], T. Mimashi[16], S. Miscetti[5], M. Mishina[8], S. Miyashita[16], N. Mondal[17], S. Mori[16], Y. Morita[16], A. Mukherjee[4], C. Newman-Holmes[4], L. Nodulman[1], R. Paoletti[11], A. Para[4], J. Patrick[4], T.J. Phillips[6], H. Piekarz[2], R. Plunkett[13], L. Pondrom[17], J. Proudfoot[1], G. Punzi[11], D. Quarrie[4], K. Ragan[10], G. Redlinger[3], J. Rhoades[17], F. Rimondi[4], L. Ristori[11], T. Rohaly[10], A. Roodman[3], A. Sansoni[5], R. Sard[7], V. Scarpine[7], P. Schlabach[7], E.E. Schmidt[4], P. Schoessow[1], M.H. Schub[12], R. Schwitters[6], A. Scribano[11], S. Segler[4], M. Sekiguchi[16], P. Sestini[11], M. Shapiro[6], M. Sheaff[17], M. Shibata[16], M. Shochet[3], J. Siegrist[9], P. Sinervo[10], J. Skarha[17], D.A. Smith[7], F.D. Snider[3], R. St.Denis[6], A. Stefanini[11], Y. Takaiwa[16], K. Takikawa[16], S. Tarem[2], D. Theriot[4], P. Tipton[9], A. Tollestrup[4], G. Tonelli[11], Y. Tsay[3], F. Ukegawa[16], D. Underwood[1], R. Vidal[4], R.G. Wagner[1], R.L. Wagner[4], J. Walsh[10], T. Watts[14], R. Webb[15], T. Westhusing[7], S. White[13], A. Wicklund[1], H.H. Williams[10], T. Yamanouchi[4], A. Yamashita[16], K. Yasuoka[16], G.P. Yeh[4], J. Yoh[4], F. Zetti[11]

[1]Argonne National Laboratory, Argonne, Illinois 60439 • [2]Brandeis University, Waltham, Massachusetts 02254 • [3]University of Chicago, Chicago, Illinois 60637 • [4]Fermi National Accelerator Laboratory, P.O. Box 500, Batavia, Illinois 60510 • [5]Laboratori Nazionali di Frascati, Instituto Nazionale do Fisica Nucleare, I-00044, Frascati, Italy • [6]Harvard University, Cambridge, Massachusetts 02138 • [7]University of Illinois, Urbana, Illinois 61801 • [8]National Laboratory for High Energy Physics (KEK), Tsukuba, Ibaraki 305, Japan • [9]Lawrence Berkeley Laboratory, Berkeley, California 94720 • [10]University of Pennsylvania, Philadelphia, Pennsylvania 19104 • [11]INFN, University and Sculoa Normale Superiore of Pisa, Pisa, Italy • [12]Purdue University, West Lafayette, Indiana 47907 • [13]Rockefeller University, New York, New York 10021 • [14]Rutgers University, Piscataway, New Jersey 08854 • [15]Texas A&M University, College Station, Texas 77843 • [16]University of Tsukuba, Tsukuba, Ibaraki 305, Japan • [17]University of Wisconsin, Madison, Wisconsin 53706

November 1989

*Submitted to Phys. Rev. D

The Two Jet Invariant Mass Distribution at $\sqrt{s} = 1.8$ TeV

F. Abe,[16] D. Amidei,[3] G. Apollinari,[11] G. Ascoli,[7] M. Atac,,[4] P. Auchincloss,[14] A. R. Baden,[6] A. Barbaro-Galtieri,[9] V. E. Barnes,[12] F. Bedeschi,[11] S. Behrends,[12] S. Belforte,[11] G. Bellettini,[11] J. Bellinger,[17] J. Bensinger,[2] A. Beretvas,[14] P. Berge,[4] S. Bertolucci,[5] S. Bhadra,[7] M. Binkley,[4] R. Blair,[1] C. Blocker,[2] J. Bofill,[4] A. W. Booth,[4] G. Brandenburg,[6] D. Brown,[6] A. Byon,[12] K. L. Byrum,[17] M. Campbell,[3] R. Carey,[6] W. Carithers,[9] D. Carlsmith,[17] J. T. Carroll,[4] R. Cashmore,[4] F. Cervelli,[11] K. Chadwick[4,12] T. Chapin,[13] G. Chiarelli,[11] W. Chinowsky,[9] S. Cihangir,[15] D. Cline,[17] D. Connor,[10] M. Contreras,[2] J. Cooper,[4] M. Cordelli,[5] M. Curatolo,[5] C. Day,[4] R. DelFabbro,[11] M. Dell'Orso,[11] L. DeMortier,[2] T. Devlin,[14] D. DiBitonto,[15] R. Diebold,[1] F. Dittus,[4] A. DiVirgilio,[11] J. E. Elias,[4] R. Ely,[9] S. Errede,[7] B. Esposito,[5] B. Flaugher,[14] E. Focardi,[11] G. W. Foster,[4] M. Franklin[6,7] J. Freeman,[4] H. Frisch,[3] Y. Fukui,[8] A. F. Garfinkel,[12] P. Giannetti ,[11] N. Giokaris,[13] P. Giromini,[5] L. Gladney,[10] M. Gold,[9] K. Goulianos,[13] C. Grosso-Pilcher,[3] C. Haber,[9] S. R. Hahn,[10] R. Handler,[17] R. M. Harris,[9] J. Hauser,[3] T. Hessing,[15] R. Hollebeek,[10] P. Hu,[14] B. Hubbard,[9] P. Hurst,[7] J. Huth,[4] H. Jensen,[4] R. P. Johnson,[4] U. Joshi,[14] R. W. Kadel,[4] T. Kamon,[15] S. Kanda,[16] D. A. Kardelis,[7] I. Karliner,[7] E. Kearns,[6] R. Kephart,[4] P. Kesten,[2] H. Keutelian,[7] S. Kim,[16] L. Kirsch,[2] K. Kondo,[16] U. Kruse,[7] S. E. Kuhlmann,[12] A. T. Laasanen,[12] W. Li,[1] T. Liss,[3] N. Lockyer,[10] F. Marchetto,[15] R. Markeloff,[17] L. A. Markosky,[17] P. McIntyre,[15] A. Menzione,[11] T. Meyer,[15] S. Mikamo,[8] M. Miller,[10] T. Mimashi,[16] S. Miscetti,[5] M. Mishina,[8] S. Miyashita,[16] N. Mondal,[17] S. Mori,[16] Y. Morita,[16] A. Mukherjee,[4] C. Newman-Holmes,[4] L. Nodulman,[1] R. Paoletti,[11] A. Para,[4] J. Patrick,[4] T. J. Phillips,[6] H. Piekarz,[2] R. Plunkett,[13] L. Pondrom,[17] J. Proudfoot,[1] G. Punzi,[11] D. Quarrie,[4] K. Ragan,[10] G. Redlinger,[3] J. Rhoades,[17] F. Rimondi,[4] L. Ristori,[11] T. Rohaly,[10] A. Roodman,[3] A. Sansoni,[5] R. Sard,[7] V. Scarpine,[7] P. Schlabach,[7] E. E. Schmidt,[4] P. Schoessow,[1] M. H. Schub,[12] R. Schwitters,[6] A. Scribano,[11] S. Segler,[4] M. Sekiguchi,[16] P. Sestini,[11] M. Shapiro,[6] M. Sheaff,[17] M. Shibata,[16] M. Shochet,[3] J. Siegrist,[9] P. Sinervo,[10] J. Skarha,[17] D. A. Smith,[7] F. D. Snider,[3] R. St.Denis,[6] A. Stefanini,[11] Y. Takaiwa,[16] K. Takikawa,[16] S. Tarem,[2] D. Theriot,[4] P. Tipton,[9] A. Tollestrup,[4] G. Tonelli,[11] Y. Tsay,[3] F. Ukegawa,[16] D. Underwood,[1] R. Vidal,[4] R. G. Wagner,[1] R. L. Wagner,[4] J. Walsh,[10] T. Watts,[14] R. Webb,[15] T. Westhusing,[7] S. White,[13] A. Wicklund,[1] H. H. Williams,[10] T. Yamanouchi,[4] A. Yamashita,[16] K. Yasuoka,[16] G. P. Yeh,[4] J. Yoh,[4] F. Zetti,[11]

[1] *Argonne National Laboratory, Argonne, Illinois 60439*
[2] *Brandeis University, Waltham, Massachusetts 02254*
[3] *University of Chicago, Chicago, Illinois 60637*
[4] *Fermi National Accelerator Laboratory, Batavia, Illinois 60510*
[5] *Laboratori Nazionali di Frascati, Istituto Nazionale di Fisica Nucleare, Frascati, Italy*
[6] *Harvard University, Cambridge, Massachusetts 02138*
[7] *University of Illinois, Urbana, Illinois 61801*
[8] *National Laboratory for High Energy Physics (KEK), Tsukuba, Ibaraki 305, Japan*
[9] *Lawrence Berkeley Laboratory, Berkeley, California 94720*
[10] *University of Pennsylvania, Philadelphia, Pennsylvania 19104*
[11] *Istituto Nationale di Fisica Nucleare, University and Scuola Normale Superiore of Pisa, Pisa, Italy*
[12] *Purdue University, West Lafayette, Indiana 47907*
[13] *Rockefeller University, New York, New York 10021*
[14] *Rutgers University, Piscataway, New Jersey 08854*
[15] *Texas A&M University, College Station, Texas 77843*
[16] *University of Tsukuba, Tsukuba, Ibaraki 305, Japan*
[17] *University of Wisconsin, Madison, Wisconsin 53706*

Abstract

We present the dijet invariant mass distribution in the region between 60 and 500 GeV, measured in 1.8 TeV $\bar{p}p$ collisions at CDF. Jets are restricted to the pseudo-rapidity interval $|\eta| < 0.7$. Data are compared with QCD calculations; axigluons are excluded with 95% confidence in the region $120 < M_A < 210$ GeV for axigluon width $\Gamma_A = N\alpha_s M_A/6$, with N=5.

The dijet invariant mass spectrum is both a testing ground for QCD and the natural place to look for new massive objects which are strongly produced and decay into two jets. In this paper, we present the invariant mass distribution of dijets produced in the process $\bar{p}p \rightarrow jet_1 + jet_2 + X$, and a limit on the production of axigluons [1], based on the 1987 CDF exposure of 26 nb^{-1}.

The CDF detector is described in detail in Ref. [2]. The components relevant to this analysis are the barrel-shaped central calorimeters which measure the electromagnetic and hadronic energy of jets. The inner electromagnetic calorimeter consists of layers of lead and scintillator, and has a resolution for electrons $\sigma/E = 13.5\%/\sqrt{E \sin\theta}$. The outer hadron calorimeter is steel and scintillator, and has a resolution for pions $\sigma/E = 70\%/\sqrt{E}$. The calorimeters are segmented into projective towers, each subtending 0.1 units of η (pseudorapidity $\eta \equiv \ln(\cot(\theta/2))$, with θ the polar angle around the proton beam direction) and 15° in ϕ (the azimuthal angle around the beam).

The data used in this analysis were taken in 1987 with hardware triggers requiring the summed transverse energy ($E \sin\theta$) in the central calorimeters to be above 20, 30, 40, and 45 GeV, depending on the luminosity. To retain the projective geometry of the detector, and to ensure full containment of jets in the central calorimeter, the collision point for each event was required to lie within 50 cm of the detector center.

About 17% of the data were rejected by this cut. Jets were identified according to the algorithm described in Ref. [3]. Briefly, local depositions of energy are identified, and all calorimeter towers with transverse energy above 0.2 GeV in a cone of radius 0.7 in $\eta - \phi$ space are collected to form the jet. The observed energy and momentum are taken to be the scalar and vector sums of the calorimeter tower energies.

For the dijet event selection, the two highest P_{T} jets in each event were required to be in the fiducial region $|\eta| < 0.7$. In addition, a cut was imposed on the azimuthal separation of the two jets, $\Delta\phi > 100°$. Trigger bias was eliminated by using only events with dijet masses in the fully efficient region, which is above 60, 65, 80, and 90 GeV for the four different trigger samples. These requirements were arrived at by considering the E_{T} trigger thresholds and the allowed η interval, and are explicated in Ref. [4].

Backgrounds from cosmic rays and accelerator losses were eliminated by requiring arrival times at the hadronic calorimeter within a 35 nsec window around the beam-beam interaction. Remaining backgrounds were timing accidentals or deposits solely in the electromagnetic calorimeter, which has no timing information, and were removed by the requirement that the electromagnetic fraction of the observed clusters (EMF) lie in the region $0.05 < \mathrm{EMF} < .95$. The validity of these background suppression schemes was checked by scanning all events with central jets with $P_{\mathrm{T}} > 100$ GeV. In 300 such events, one real jet event was lost, and two bad events (P_{T} approximately 100 GeV) were passed.

The energy and momentum of each jet were corrected independently for losses due to cracks, leakage, and nonlinear response of the calorimeter according to a detector simulation and the ISAJET Monte Carlo [5]. The ISAJET jet fragmentation properties have been checked against charged particle properties measured in the CDF

jet data, and the calorimeter simulation has been tuned to the observed response for isolated charged pions in minimum-bias $\bar{p}p$ interactions in CDF, and test beam data. As determined from the Monte Carlo, the total loss of jet energy from all effects ranges from 30% for 30 GeV jets to 14% at 200 GeV. By varying the fragmentation parameters and the calorimeter response in the simulation, we estimate the uncertainty in the jet energy scale to be 9% at 30 GeV and 5% at 200 GeV. The dijet invariant mass, M, is defined as $\sqrt{(E_1 + E_2)^2 - (P_1 + P_2)^2}$, where E_i and P_i are the corrected energy and momenta of the two central jets. The dijet mass resolution (σ(M)) as determined from the Monte Carlo is shown in Fig. 1; the fractional resolution (σ/M) varies from 15% at 60 GeV to 10% at 400 GeV. Fits to two plausible functional forms for the resolution are also shown in Fig. 1. These are of the form $\sigma = \alpha\sqrt{M} + \beta M$ and $\sigma = \alpha\sqrt{M} + \beta$.

The resulting dijet invariant mass spectrum was then corrected for the smearing (or feed-up) effect caused by the finite mass resolution of the detector. The procedure was to convolve a test function of the form $Am^{-\alpha}e^{\beta m}$ with the dijet mass resolution and then fit to the data. For the best fit parameters, the ratios of the unsmeared to the smeared test functions, integrated over the data bins, were applied to the data. These correction factors range from 0.85 at 60 GeV to 0.9 above 200 GeV.

In Table 1 and Fig. 2 we present the corrected CDF dijet mass spectrum at $\sqrt{s}$ = 1800 GeV, compared with a range of theoretical predictions [7]. The result of UA2 at $\sqrt{s}$ = 540 GeV [6] is also shown. In the figure, the uncertainties include the statistical uncertainties and the mass-dependent part of the systematic uncertainties. These systematic cross-section uncertainties, including the uncertainty in the jet energy scale (45% of the cross section at 60 GeV and 30% at 400 GeV), the resolution deconvolution (10%), and the integrated luminosity (15%), range from 48% at 60 GeV

to 35% at 400 GeV. The solid lines are the envelopes of several QCD calculations with the structure functions D01, D02 [8], EHLQ1, EHLQ2 [9], and the momentum scales $Q = P_T$ and $P_T/2$. Our measurement and QCD are consistent within experimental and theoretical uncertainties.

The dijet invariant mass distribution, at both the theoretical and experimental level, is sensitive to the presence of additional jets in the event, through both event selection and definition of invariant mass. Restricting the sample to more "back-to-back" events ($\Delta\phi > 150°$) lowered the measured cross-section roughly 20%. Merging nearby jets, within an η-ϕ radius of 1.2 (1.5) from the leading two jets, resulted in a cross-section 30% (85%) higher. These effects, inherent to QCD [10], are not included in the systematic uncertainty reported for the cross section.

Recently, chiral models of QCD with the symmetry group $SU(3)_L \times SU(3)_R$ have been proposed [1] in which the symmetry is broken to $SU(3)_V$ and as a consequence the axial vector gauge particles, axigluons, become massive. Bagger, Schmidt, and King [11] (B-S-K) have calculated the contribution of axigluons to the jet production cross-sections assuming an axigluon width $\Gamma_A = N\alpha_s M_A/6$, with N being proportional to the number of decay channels (light quarks), α_s the strong coupling constant, and M_A the axigluon mass. They have ruled out the mass region $125 < M_A < 275$ GeV based on the UA1 jet P_T spectrum at $\sqrt{s} = 630$ GeV [12]. UA1 [13] has excluded masses between 110 and 310 GeV for an axigluon width $\Gamma_A < 0.4\,M_A$ (equivalent to N=24 for α_s=0.1), using an incoherent sum of dijet and axigluon cross-sections. We have repeated the B-S-K calculation at the Tevatron energy with EHLQ2 and $Q = P_T$ using a coherent sum of amplitudes. EHLQ2 was chosen because it gave the most conservative limits. For the axigluon analysis, we have compared to the data without the application of smearing corrections, and instead have added the effect

of mass resolution to the theoretical predictions. The data and the calculations are shown in Fig. 3, where the predicted spectra have been normalized to the data in the region $60 < M_{JJ} < 120$ GeV.

The χ^2 for a fit including an axigluon is calculated for the three or four bins under the axigluon bump depending on the mass and width of the axigluon, after normalization to the low mass region. To take into account the uncertainty in the jet energy scale, we have allowed both edges of each data bin to vary and have used the smallest χ^2 to set a limit. At the 95% confidence limit, axigluons are excluded in the mass intervals: $120 < M_A < 210$ GeV for $N = 5$ ($\Gamma_A = 0.09 M_A$), and $120 < M_A < 150$ GeV for $N = 10$ ($\Gamma_A = 0.18 M_A$).

Although CDF data on dijet mass extend the range explored at the $Sp\bar{p}S$, our sensitivity to axigluon masses below 300 GeV is lessened by the predominance of gluon-gluon and gluon-quark scattering in this region, and the fact that axigluon production proceeds via $q\bar{q}$ scattering. The higher statistics of the 1988-89 Tevatron run will extend our sensitivity to larger axigluon masses.

This work has been made possible by the construction and successful operation of the Tevatron collider by the Fermilab Accelerator Division. We thank J. Bagger, C. Schmidt, S. King, and E. Eichten for providing help with the theoretical calculations. This work is supported in part by the U.S. Department of Energy and National Science Foundation; the Italian Istituto Nazionale di Fisica Nucleare; the Ministry of Science, Culture, and Education of Japan; and the A. P. Sloan Foundation.

References

[1] P. H. Frampton and S. L. Glashow, Phys. Lett. 190B (1987) 157.

[2] F. Abe et al., CDF Collaboration, Nucl. Instr. and Meth. A271 (1988) 387.

[3] F. Abe et al., CDF Collaboration, Phys. Rev. Lett. 62 (1989) 613.

[4] Y. D. Tsai, Ph.D. thesis, the Univ. of Chicago, 1989 (unpublished).

[5] F. E. Paige and S. D. Protopopescu, Brookhaven National Laboratory Report BNL-37066, 1985.

[6] P. Bagnaia et al., UA2 Collaboration, Phys. Lett. 138B (1984) 430.

[7] Program to calculate the dijet mass spectrum was provided by J. Bagger, C. Schmidt, and S. King. Routines for strong coupling constant and structure functions were provided by E. Eichten.

[8] D.W. Duke and J.F. Owens, Phys. Rev. D30 (1984) 49.

[9] E. Eichten, I. Hinchliffe, K. Lane, and C. Quigg, Rev. Mod. Phys. 56 (1984) 579.

[10] S. Ellis, Z. Kunszt, and D. Soper, Phys. Rev. Lett. 62 (1989) 726.

[11] J. Bagger, C. Schmidt, and S. King, Phys. Rev. D37 (1988) 1188.

[12] G. Arnison et al., UA1 Collaboration, Phys. Lett. 172B (1986) 461.

[13] C. Albajar et al., UA1 Collaboration, Phys. Lett. 209B (1988) 127.

Fig. 1 The dijet mass resolution as determined from Monte Carlo simulation. A cluster cone size of 0.7 in $\eta - \phi$ and a tower E_T threshold of 0.2 GeV are used. Both jets were restricted to the fiducial region $|\eta| \leq 0.7$. Two fits are shown: $\sigma = 0.68\sqrt{M} + 0.065M$ (solid line) and $\sigma = 2.229\sqrt{M} - 8.40$ (dotted line).

Fig. 2 The dijet mass spectra at $\sqrt{s} = 1800$ GeV (CDF) and $\sqrt{s} = 540$ GeV (UA2). The uncertainties include the statistical uncertainties and the mass dependent systematic uncertainties. The additional CDF (UA2) mass independent normalization uncertainty of 35% (45%) is shown in the key. The two pairs of solid lines are the envelopes of QCD calculations ($2 \rightarrow 2$) with the structure functions DO1, DO2, EHLQ1 and EHLQ2, and the momentum scales $Q = P_T/2$ and P_T.

Fig. 3 The CDF dijet mass spectrum (uncorrected for mass resolution) compared with calculations involving the effect of axigluons, for two values of the axigluon width parameter, N. Predictions for axigluon masses of 200, 300 and 400 GeV are shown; these predictions have been normalized to the data in the region $60 < M_{JJ} < 120$ GeV.

Table 1: The dijet mass spectrum. Jets are restricted to the pseudorapidity region $|\eta| < 0.7$.

M_{JJ} (GeV)	$d\sigma/dM_{JJ}$ (nb/GeV)	Sys. Error	Stat. Error
62.5	37.8	18.5	4.4
67.5	25.5	12.0	0.62
72.5	17.7	8.0	0.52
77.5	13.2	5.8	0.45
82.5	9.39	4.0	0.31
87.5	6.46	2.70	0.26
92.5	5.44	2.22	0.21
97.5	4.17	1.68	0.18
105.5	2.83	1.11	0.11
115.5	1.72	0.65	0.083
125.5	1.17	0.43	0.068
135.5	0.756	0.275	0.055
145.5	0.569	0.204	0.048
157.5	0.321	0.113	0.029
172.5	0.247	0.085	0.026
189.5	0.121	0.041	0.016
210.5	0.0708	0.0237	0.0120
230.5	0.0445	0.0147	$+0.0117$
			-0.0076
254.5	0.0230	0.0075	$+0.0070$
			-0.0043
284.5	0.0122	0.0040	$+0.0056$
			-0.0029
323.5	0.00731	0.00237	$+0.00334$
			-0.00171
373.5	0.00244	0.00080	$+0.00237$
			-0.00074
423.5	0.00244	0.00081	$+0.00237$
			-0.00074
494.5	0.000404	0.000139	$+0.000929$
			-0.000118

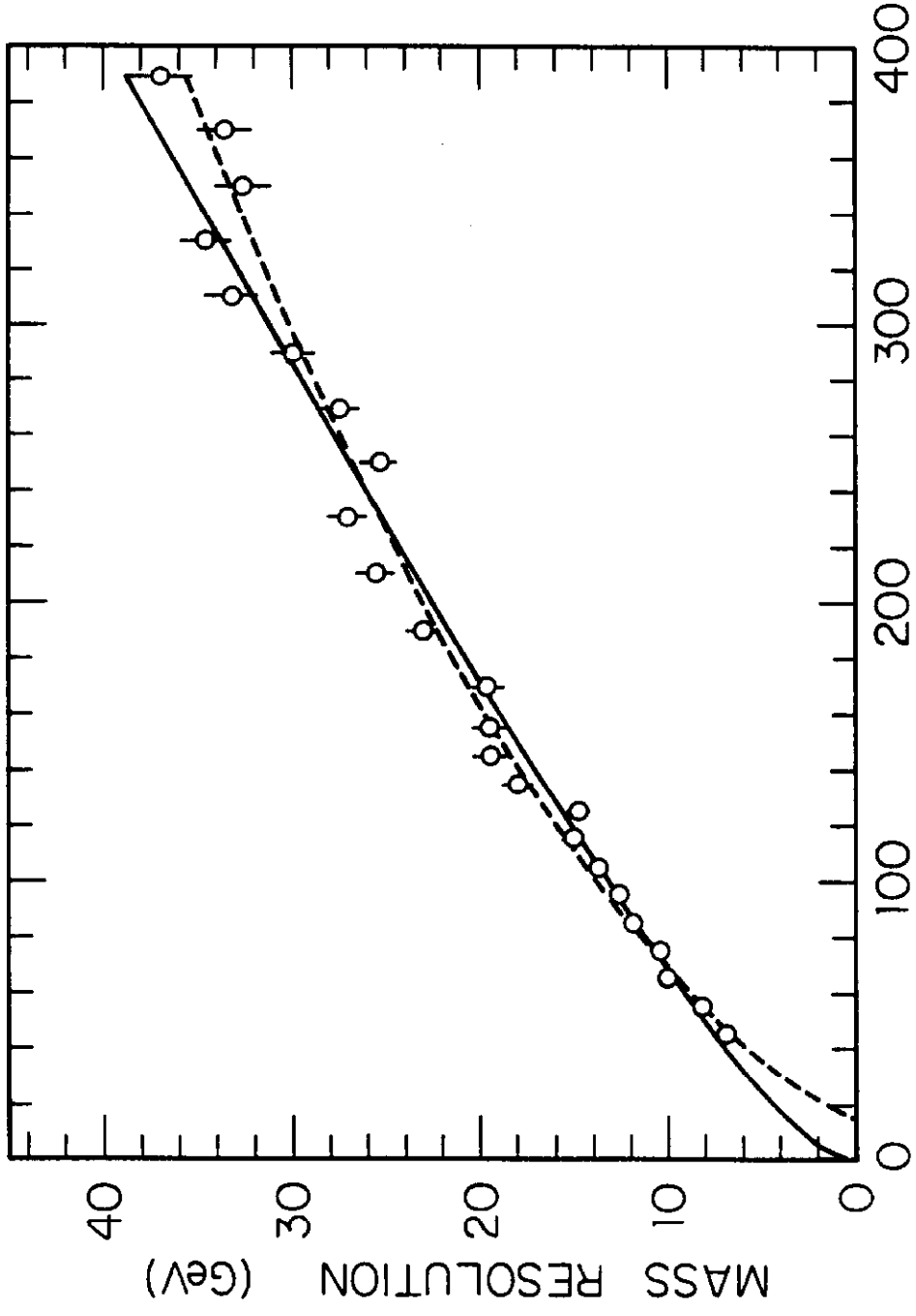
MASS RESOLUTION (GeV)
0
10
20
30
40
0
100
200
300
400
DIJET MASS (GeV)

Figure 1.

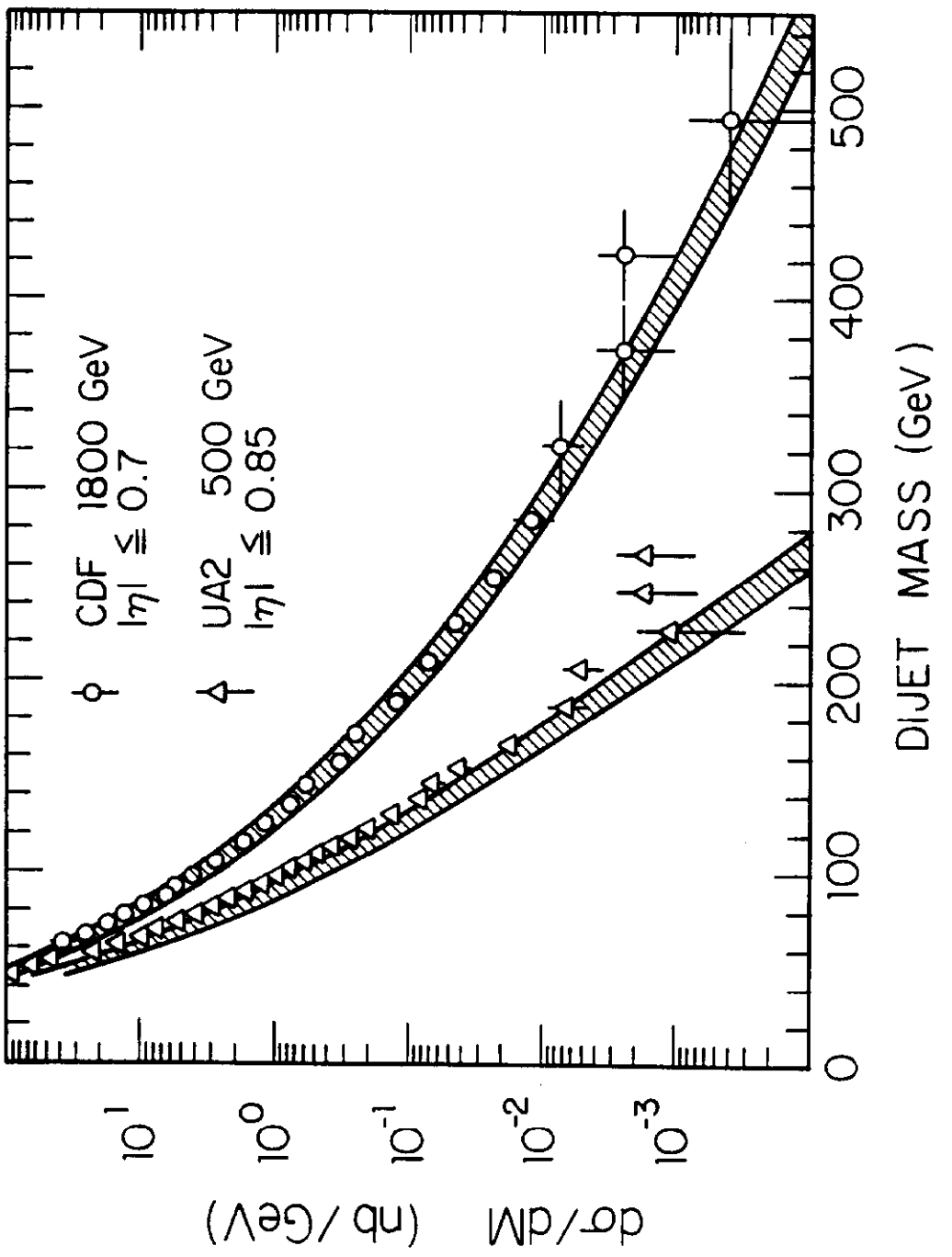
CDF 1800 GeV
|η| ≤ 0.7
UA2 500 GeV
|η| ≤ 0.85
dσ/dM (nb/GeV)
DIJET MASS (GeV)
10^1
10^0
10^-1
10^-2
10^-3
0
100
200
300
400
500

Figure 2.

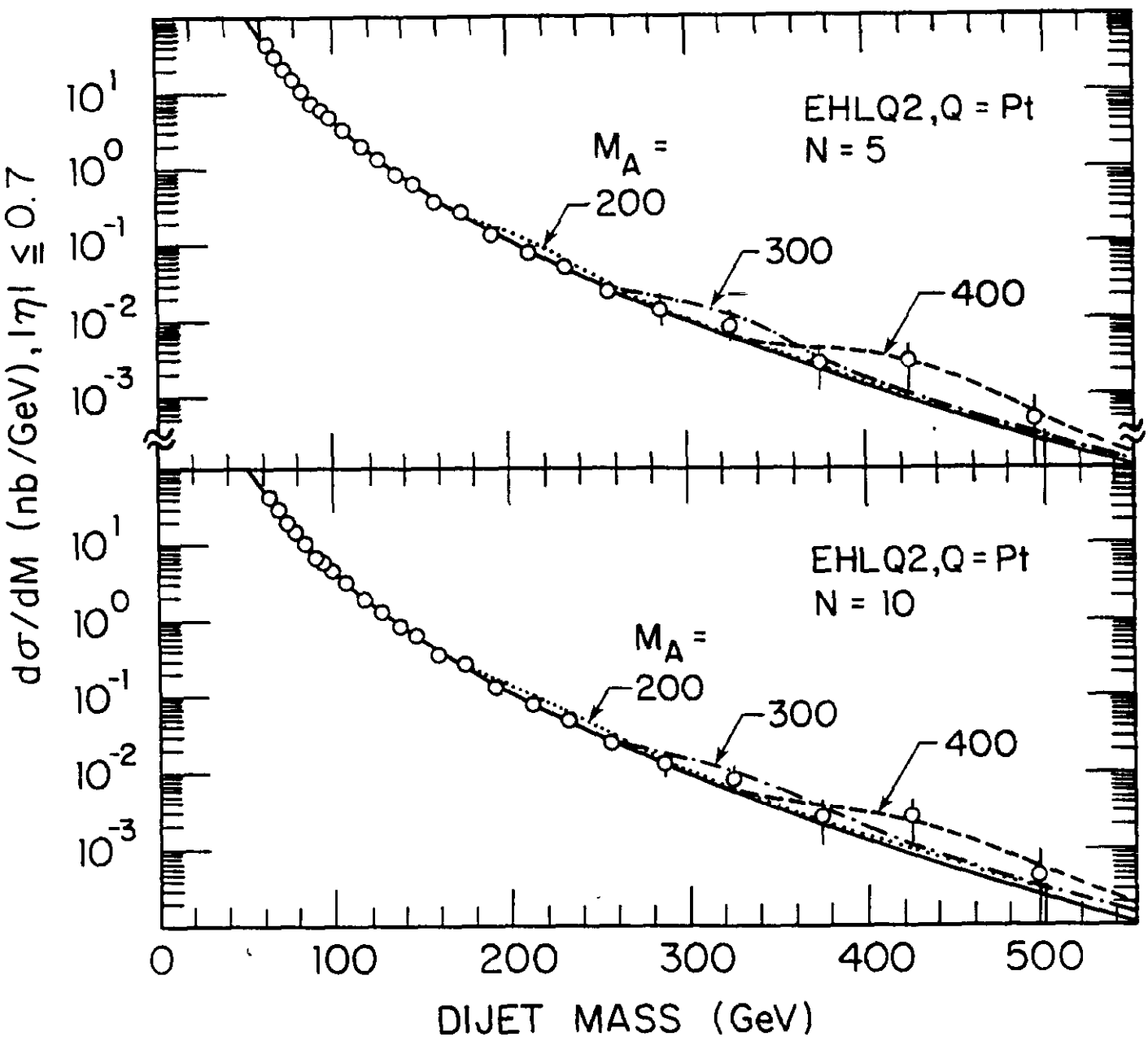
EHLQ2,Q = Pt
N = 5
M_A =
200
300
400
EHLQ2,Q = Pt
N = 10
M_A =
200
300
400
$d\sigma/dM$ (nb/GeV), $|\eta| \leq 0.7$
10^1
10^0
10^{-1}
10^{-2}
10^{-3}
0
100
200
300
400
500
DIJET MASS (GeV)

Figure 3.